AIAA JOURNAL
Vol. 46, No. 4, April 2008

Technical Notes

TECHNICAL NOTES are short manuscripts describing new developments or important results of a preliminary nature. These Notes should not exceed 2500 words (where a figure or table counts as 200 words). Following informal review by the Editors, they may be published within a few months of the date of receipt. Style requirements are the same as for regular contributions (see inside back cover).

Analytical Equilibrium Swirling Inflow Conditions for Computational Fluid Dynamics

Xi Jiang,* George A. Siamas,† and Luiz C. Wrobel‡
Brunel University,
Uxbridge, England UB8 3PH, United Kingdom

DOI: 10.2514/1.29439

I. Introduction

THE specification of swirling inflow conditions is an integral and important part of computational fluid dynamics (CFD) of swirling flows, which are complex flows with many practical applications [1], for instance, in turbulent combustion [2]. To specify a swirling velocity profile with a desired swirl number in a traditional CFD analysis based on a Reynolds-averaged Navier–Stokes (RANS) modeling approach is not an easy task, which becomes even more difficult in advanced CFD approaches such as direct numerical simulation (DNS) or large-eddy simulation (LES). DNS or LES of spatially inhomogeneous turbulent flows requires turbulent inflow boundary conditions [3], which may be generated either from an auxiliary simulation, from a proper orthogonal decomposition and linear stochastic estimation [4], from a digital filter reproducing specified statistical data [5], or simply taken as the mean velocity profile with superimposed fluctuations [6], which is essentially a perturbed inflow. With the presence of swirling, inflow conditions are difficult to specify. For RANS-based CFD, an appropriate mean velocity profile is needed. For DNS and LES, apart from the mean velocity profile, information on an appropriate "turbulent" component is needed as well.

Pierce and Moin [7] developed a method for generating equilibrium swirling inflow conditions, which represents a logical, idealized starting point for generating swirling velocity profiles. In their method, the swirling inflow is obtained numerically by solving for the flow driven by fictitious axial and azimuthal body forces, where the axial body force represents the mean pressure gradient that drives the physical flow. The azimuthal body force is not physically producible and may be thought of as existing only to overcome drag from the walls. This technique was used in LES of a coaxial jet combustor and good agreement with the experimental data was observed [7]. The method can be regarded as an effective and simple means of generating realistic swirling inflow conditions.

Received 22 December 2006; revision received 6 November 2007; accepted for publication 6 December 2007.

*Senior Lecturer, Mechanical Engineering, School of Engineering and Design.
†Ph.D. Researcher, Mechanical Engineering, School of Engineering and Design.
‡Professor, Mechanical Engineering, School of Engineering and Design.

In this study, efforts have been made to derive an analytical form of the equilibrium swirling inflow conditions. The analytical swirling inflow is easy to implement, as it does not require solving for the flow numerically [7]. The particular forms of the analytical equilibrium swirling velocity profiles have been obtained for swirling annular and round jets, which can be directly applied in the specification of swirling inflow conditions for RANS approaches and further explored for the specification of swirling inflow conditions for DNS and LES, regardless of the turbulent component needed in the time-dependent simulations. A desired swirl number at the inflow can also be conveniently achieved by adjusting a constant.

II. Analytical Equilibrium Swirling Inflow Conditions

For stationary, axisymmetric, parallel flow, the axial and azimuthal momentum equations with body forces are [7]

$$\frac{1}{r}\frac{\mathrm{d}}{\mathrm{d}r}(r\tau_{xr}) + f_x = 0, \qquad \frac{1}{r}\frac{\mathrm{d}}{\mathrm{d}r}(r\tau_{r\theta}) + \frac{\tau_{r\theta}}{r} + f_\theta = 0 \tag{1}$$

where the shear stresses are given by

$$\tau_{xr} = \mu\left(\frac{\partial u_r}{\partial x} + \frac{\partial u_x}{\partial r}\right), \qquad \tau_{r\theta} = \mu\left(\frac{\partial u_\theta}{\partial r} + \frac{1}{r}\frac{\partial u_r}{\partial \theta} - \frac{u_\theta}{r}\right) \tag{2}$$

In Eqs. (1) and (2), x, r, and θ represent the axial, radial, and azimuthal directions, respectively, f_x and f_θ represent the body forces [7], τ represents shear stress, and μ represents dynamic viscosity.

For a swirling inflow, one can assume $u_r = 0$, and the shear stresses in turn become

$$\tau_{xr} = \mu\frac{\mathrm{d}u_x}{\mathrm{d}r}, \qquad \tau_{r\theta} = \mu\left(\frac{\mathrm{d}u_\theta}{\mathrm{d}r} - \frac{u_\theta}{r}\right) \tag{3}$$

Substituting Eq. (3) into Eq. (1), and after some manipulation, we have

$$\frac{\mathrm{d}^2u_x}{\mathrm{d}r^2} + \frac{1}{r}\frac{\mathrm{d}u_x}{\mathrm{d}r} + \frac{f_x}{\mu} = 0, \qquad \frac{\mathrm{d}^2u_\theta}{\mathrm{d}r^2} + \frac{1}{r}\frac{\mathrm{d}u_\theta}{\mathrm{d}r} - \frac{u_\theta}{r^2} + \frac{f_\theta}{\mu} = 0 \tag{4}$$

The analytical solutions of u_x and u_θ in Eq. (4) can be obtained as

$$u_x = -\frac{1}{4}\frac{f_x}{\mu}r^2 + C_1\ln r + C_2, \qquad u_\theta = -\frac{1}{3}\frac{f_\theta}{\mu}r^2 + C_3 r + \frac{C_4}{r} \tag{5}$$

where C_1, C_2, C_3, and C_4 are constants specified by the physical conditions, while f_x and f_θ are specified by appropriate physical conditions such as the maximum velocity at the inflow. Note that Eq. (5) cannot be used at $r = 0$ and in a practical simulation one can always assume a very small value of r instead. The physical conditions that can be used to define these constants are problem dependent. For swirling annular and round jets, these constants can be defined by the possible physical conditions.

III. Specification of the Equilibrium Swirling Inflow Conditions

Swirling inflow is commonly related to two flow configurations: a round jet with an axisymmetric shear layer and an annular jet with

two adjacent axisymmetric shear layers. The "axisymmetric" configuration referred to herein includes an azimuthal motion associated with the swirling velocity. For the annular and round jets, the constants C_1, C_2, C_3, C_4, f_x, and f_θ in Eq. (5) can be defined according to the relevant physical conditions as follows.

A. Annular Jet

For an annular jet with inner and outer radii R_i and R_o, nonslip conditions at the inner and outer radii can be used to define the constants C_1, C_2, C_3, and C_4. Taking $u_x = u_\theta = 0$ at $r = R_i$ and $r = R_o$, from Eq. (5), C_1, C_2, C_3, and C_4 can be calculated as

$$C_1 = \frac{f_x\left(R_i^2 - R_o^2\right)}{4\mu(\ell_n R_i - \ell_n R_o)}, \qquad C_2 = \frac{-f_x\left(R_i^2\,\ell_n R_o - R_o^2\,\ell_n R_i\right)}{4\mu(\ell_n R_i - \ell_n R_o)}$$
$$C_3 = \frac{f_\theta\left(R_i^2 + R_i R_o + R_o^2\right)}{3\mu(R_i + R_o)}, \qquad C_4 = \frac{-f_\theta R_i^2 R_o^2}{3\mu(R_i + R_o)} \tag{6}$$

Consequently, the swirling velocity inflow profiles for an annular jet can be written as

$$u_x = -\frac{1}{4}\frac{f_x}{\mu}\left(r^2 - \frac{R_i^2 - R_o^2}{\ell_n R_i - \ell_n R_o}\ell_n r + \frac{R_i^2\,\ell_n R_o - R_o^2\,\ell_n R_i}{\ell_n R_i - \ell_n R_o}\right)$$
$$u_\theta = -\frac{1}{3}\frac{f_\theta}{\mu}\left(r^2 - \frac{R_i^2 + R_i R_o + R_o^2}{R_i + R_o}r + \frac{R_i^2 R_o^2}{R_i + R_o}\frac{1}{r}\right) \tag{7}$$

In Eq. (7), f_x and f_θ can be defined by the maximum velocities at the inflow boundary. For the sake of convenience, a unit maximum velocity may be assumed for u_x (which is often the case if a nondimensional form of the governing equations is employed). For the annular jet, from Eq. (7),

$$f_x = -\frac{8\mu(\ell_n R_o - \ell_n R_i)}{R_o^2 - R_i^2 + R_i^2\,\ell_n\left[\frac{R_i^2 - R_o^2}{2(\ell_n R_i - \ell_n R_o)}\right] - R_o^2\,\ell_n\left[\frac{R_i^2 - R_o^2}{2(\ell_n R_i - \ell_n R_o)}\right] - 2R_i^2\,\ell_n R_o + 2R_o^2\,\ell_n R_i}$$

leads to $u_{x,\max} = 1$ at

$$r = \sqrt{\frac{R_i^2 - R_o^2}{2(\ell_n R_i - \ell_n R_o)}}$$

The parameter f_θ in Eq. (7) will define the degree of swirling in the flow, as discussed in Sec. III.C.

Figure 1 shows the sample velocity profiles given in Eq. (7), where a unit value has been assumed for R_o and μ for simplicity. In this figure, distributions of u_x/f_x and u_θ/f_θ between (R_i, R_o) have been shown for different values of R_i. It can be seen that u_x/f_x and u_θ/f_θ show similar trends.

B. Round Jet

For a round jet with symmetry, $C_1 = 0$ may be used due to the symmetry condition $\mathrm{d}u_x/\mathrm{d}r|_{r=0} = 0$ (it can be shown that

$$\frac{\mathrm{d}u_x}{\mathrm{d}r} = -\frac{1}{2}\frac{f_x}{\mu}r + \frac{1}{r}C_1$$

in this case). It is also reasonable to take $C_4 = 0$ due to the fact that $u_\theta = 0$ at $r = 0$. Assuming that the jet velocity becomes zero at a radial location $r = R_o$, C_1, C_2, C_3, and C_4 can be calculated as

$$C_1 = 0, \qquad C_2 = \frac{f_x R_o^2}{4\mu}, \qquad C_3 = \frac{f_\theta R_o}{3\mu}, \qquad C_4 = 0 \tag{8}$$

Consequently the swirling velocity inflow profiles for a round jet can be written as

$$u_x = -\frac{1}{4}\frac{f_x}{\mu}\left(r^2 - R_o^2\right), \qquad u_\theta = -\frac{1}{3}\frac{f_\theta}{\mu}(r^2 - R_o r) \tag{9}$$

In Eq. (9), f_x and f_θ can also be defined by the maximum velocities at the inflow boundary. For instance, a unit maximum velocity for u_x may be assumed (which is often the case if a nondimensional form of the governing equations is employed). For the round jet, from Eq. (9), $f_x = 4\mu/R_o^2$ leads to $u_{x,\max} = 1$ at $r = 0$. The parameter f_θ in Eq. (9) will define the flow swirling, as discussed in the next section.

Figure 2 shows the velocity profiles given in Eq. (9), where a unit value has been assumed for R_o and μ. It can be seen that u_x/f_x reaches a maximum value at $r = 0$ which is the jet centerline while u_θ/f_θ reaches a maximum value at $r = R_o/2$.

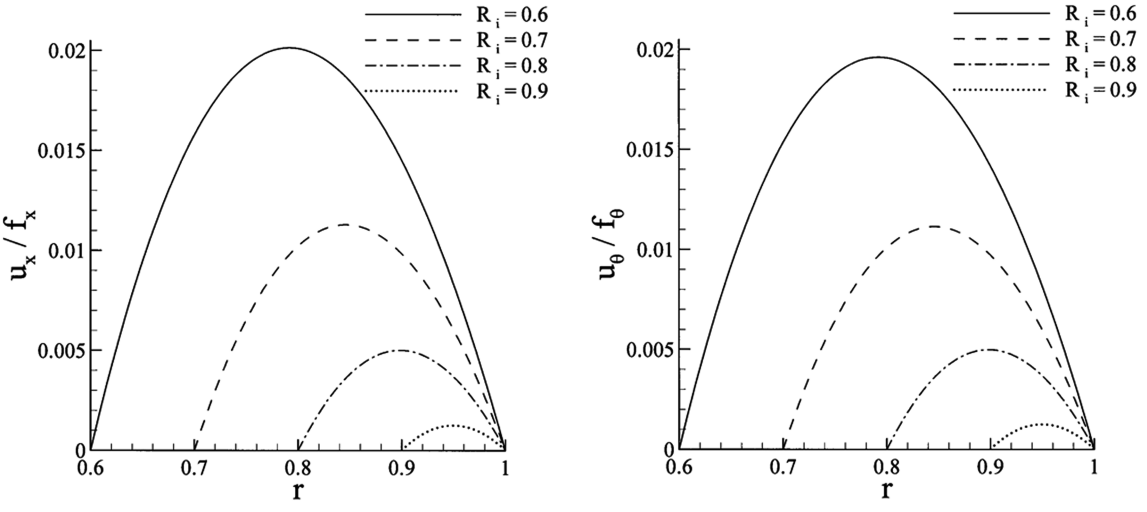

Fig. 1 Sample velocity profiles of an equilibrium swirling inflow for an annular jet with $R_o = 1$ and $\mu = 1$.

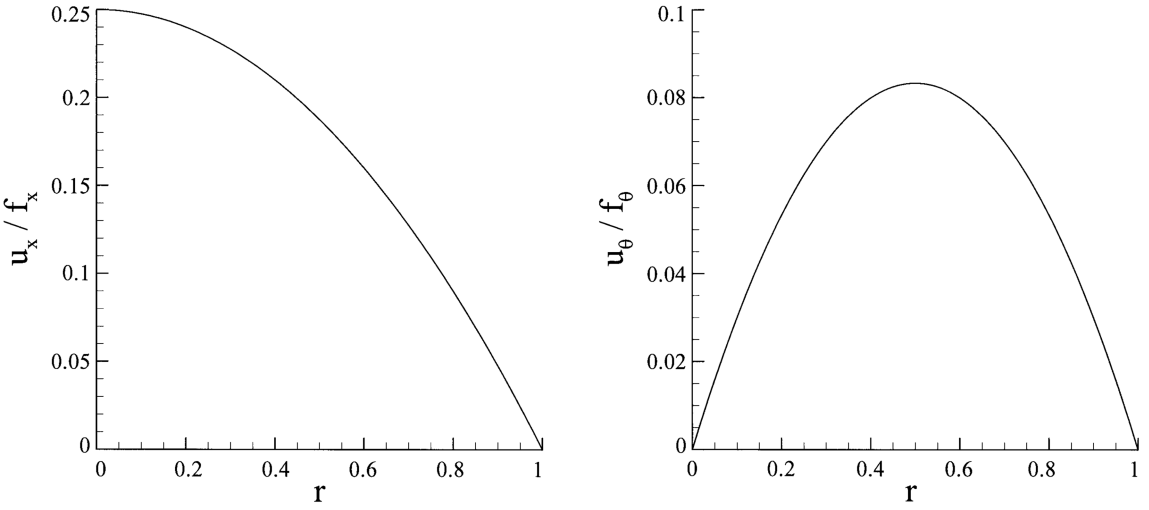

Fig. 2 Velocity profiles of an equilibrium swirling inflow for a round jet with $R_o = 1$ and $\mu = 1$.

C. Swirl Number

The swirl number can be calculated as

$$S = \frac{\int_{R_i}^{R_o} u_x u_\theta r^2 \, \mathrm{d}r}{R_o \int_{R_i}^{R_o} u_x^2 r \, \mathrm{d}r} \tag{10}$$

For known u_x and u_θ, the swirl number can be conveniently calculated from the above definition. A certain swirl number can be achieved by adjusting the constant body force term f_θ. From Eqs. (7) and (9), it can be observed that the swirl number is a simple linear function of f_θ for annular and round jets. In a practical simulation, a certain degree of swirling can be conveniently achieved by varying f_θ in Eqs. (7) and (9), that is, $f_\theta = 0$ leads to no swirling in the flow and a large f_θ leads to a strong swirling in the flowfield.

IV. Validation

The axial and azimuthal inflow velocity profiles for a swirling annular jet are compared with experimental results and simulation data obtained from the commercial CFD package Fluent using the methods described by Vanierschot and Van den Bulck [8]. The experimental data of Sheen et al. [9] and Vanierschot and Van den Bulck [10] are used for comparison with the analytical velocity distributions obtained herein. Figure 3 shows the comparison between the analytical swirling velocity profiles with those obtained from experimental data [9,10] and Fluent simulation at axial locations very close to the jet nozzle exit. For a consistent comparison, the velocities and distances in Fig. 3 have been normalized by the maximum mean axial velocity and outer radius of the jet nozzle exit, while the body forces f_x and f_θ have been adjusted to match the experimental conditions. The agreements of the theoretical predictions with both the experimental results and Fluent simulation are satisfactory, validating the effectiveness of the analytical swirling inflow conditions described in this study. The analytical swirling inflow condition has also been used in our ongoing DNS of a swirling gas–liquid annular jet. Figure 4 shows sample velocity vector plots at two different streamwise locations, where $z = 2.0$ corresponds to an upstream cross section and $z = 4.0$ corresponds to a downstream cross section in the flow domain where swirling was applied at the jet nozzle exit $z = 0$. The DNS results clearly indicate the swirling flow pattern which is not self-sustaining [7] and which is evolving into very complex flow structures at downstream locations.

V. Conclusions

Analytical swirling inflow conditions have been examined for swirling annular and round jets. Based on the equilibrium swirling inflow concept of Pierce and Moin [7], the analytical form of the axial and azimuthal velocity components has been given in Eqs. (7) and (9) for annular and round jets, respectively. Without solving for the flow numerically, the analytical swirling inflow is easy to implement in a

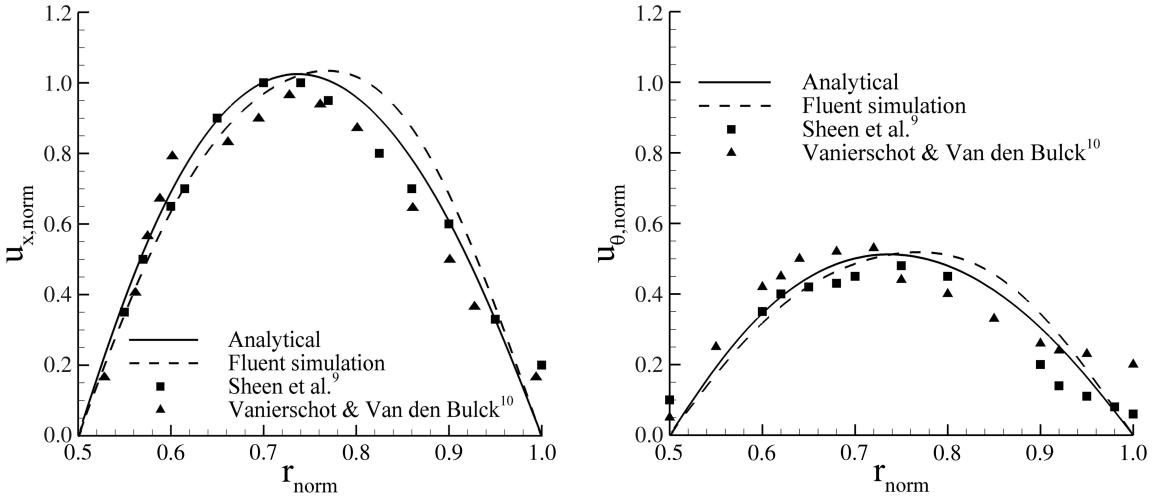

Fig. 3 Radial profiles of axial and azimuthal velocities very close to the jet nozzle exit.

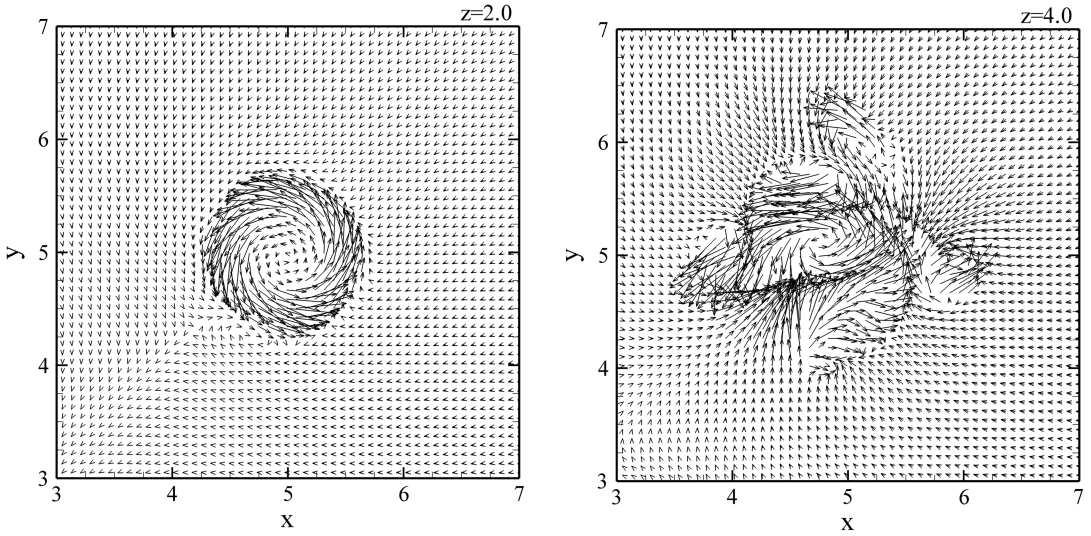

Fig. 4 Sample velocity vectors from DNS of a swirling gas–liquid annular jet with swirl number 0.4.

CFD simulation. The analytical swirling inflow conditions provided can be directly applied in RANS-based CFD simulations, while they can also be used as the mean velocity profile for advanced CFD techniques such as DNS and LES. For annular and round jets, a certain swirl number at the inflow can be conveniently setup by varying the body force f_θ in Eqs. (7) and (9), with which the swirl number has a linear dependence. The analytical solution is in good agreement with experimental and simulation results, indicating the effectiveness of the swirling inflow conditions proposed.

References

[1] Shtern, V., and Hussain, F., "Collapse, Symmetry Breaking, and Hysteresis in Swirling Flows," *Annual Review of Fluid Mechanics*, Vol. 31, Jan. 1999, pp. 537–566. doi:10.1146/annurev.fluid.31.1.537

[2] Sloan, D. G., Smith, P. J., and Smoot, L. D., "Modeling of Swirl in Turbulent-Flow Systems," *Progress in Energy and Combustion Science*, Vol. 12, No. 3, 1986, pp. 163–250. doi:10.1016/0360-1285(86)90016-X

[3] Klein, M., Sadiki, A., and Janicka, J., "A Digital Filter Based Generation of Inflow Data for Spatially Developing Direct Numerical or Large Eddy Simulations," *Journal of Computational Physics*, Vol. 186, No. 2, 2003, pp. 652–665. doi:10.1016/S0021-9991(03)00090-1

[4] Druault, P., Lardeau, S., Bonnet, J.-P., Coiffet, F., Delville, J., Lamballais, E., Largeau, J. F., and Perret, L., "Generation of Three-Dimensional Turbulent Inlet Conditions for Large-Eddy Simulation," *AIAA Journal*, Vol. 42, No. 3, 2004, pp. 447–456.

[5] di Mare, L., Klein, M., Jones, W. P., and Janicka, J., "Synthetic Turbulence Inflow Conditions for Large-Eddy Simulation," *Physics of Fluids*, Vol. 18, No. 2, 2006, pp. 1–11.

[6] Jiang, X., Zhao, H., and Luo, K. H., "Direct Computation of Perturbed Impinging Hot Jets," *Computers and Fluids*, Vol. 36, No. 2, 2007, pp. 259–272. doi:10.1016/j.compfluid.2006.01.015

[7] Pierce, C. D., and Moin, P., "Method for Generating Equilibrium Swirling Inflow Conditions," *AIAA Journal*, Vol. 36, No. 7, 1998, pp. 1325–1327.

[8] Vanierschot, M., and Van den Bulck, E., "Numerical Study of Hysteresis in Annular Swirling Jets with a Stepped-Conical Nozzle," *International Journal for Numerical Methods in Fluids*, Vol. 54, No. 3, 2007, pp. 313–324. doi:10.1002/fld.1400

[9] Sheen, H. J., Chen, W. J., and Jeng, S. Y., "Recirculation Zones of Unconfined and Confined Annular Swirling Jets," *AIAA Journal*, Vol. 34, No. 3, 1996, pp. 572–579.

[10] Vanierschot, M., and Van den Bulck, E., "Hysteresis in Flow Patterns in Annular Swirling Jets," *Experimental Thermal and Fluid Science*, Vol. 31, No. 6, 2007, pp. 513–524. doi:10.1016/j.expthermflusci.2006.06.001

K. Ghia
Associate Editor